GEOLOŠKI ANALI BALKANSKOGA POLUOSTRVA
Volume 86 (2), December 2025, 73-85
–
https://doi.org/10.2298/GABP2511010I
Original scientific paper
Оригинални научни рад

Structural data acquisition in a cave using smartphone LiDAR and Virtual Compass

Igor Ivanovski[1], Gorgi Dimov[1], Ivan Boev[1], Sonja Lepitkova[1] & Gose Petrov[1]

Abstract. Three-dimensional (3D) modeling has become a preferred approach for acquiring high-accuracy spatial data efficiently. While terrestrial laser scanning (TLS) delivers high-quality point clouds, its cost often motivates the search for affordable alternatives. In structural geology, robust rock-mass characterization requires geometric information from both intact rock and its discontinuities; point-cloud–based surface analysis enables estimation of key parameters such as dip and dip direction. Recent smartphones equipped with LiDAR sensors offer a low-cost means to obtain 3D point clouds suitable for such analyses. This study evaluates the capability of an iPhone Pro LiDAR scanner to acquire structural data from planar features inside a cave in southern part of Macedonia and compares the results with conventional compass measurements. It represents the next step in verification of this methodology, previously performed on various outcrops in Macedonia. The 3D point clouds were processed in CloudCompare software, and structural orientations were derived using its Virtual Compass tool. The smartphone-based measurements on a 3D point cloud using Virtual Compass, show a highly promising agreement with the geological compass data, indicating that mobile LiDAR can provide a reliable and efficient complement to traditional field methods for cave environments and similarly constrained settings.

Key words:
Compass; LiDAR, point cloud, iPhone, cave.

Апстракт. Тродимензионално (3D) моделовање постало је преферирани приступ за ефикасно прикупљање просторно врло прецизних података. Иако терестричко ласерско скенирање (TLS) обезбеђује висококвалитетне облаке тачака, његова цена често подстиче потребу за приступачнијим алтернативама. У структурној геологији, поуздана карактеризација стенске масе захтева геометријске информације и о интактној стени и о њеним дисконтинуитетима; анализа површина заснована на облацима тачака омогућава процену кључних параметара као што су пад и правац пада. Новији паметни телефони опремљени LiDAR сензорима нуде нискобуџетни начин добијања 3D облака тачака погодних за овакве анализе. Ова студија процењује могућности LiDAR скенера iPhone Pro уређаја за прикупљање структурних података са равних површина унутар пећине на југу Македоније и упоређује резултате са конвенционалним мерењима компасом. Представља наредни корак у верификацији ове методологије, претходно примењене на различитим из-

[1]Faculty of Natural and Technical Sciences, University "Goce Delčev" - Štip, Blvd. "Goce Delčev" 89 MK-2000, Republic of Macedonia;
E-mail: igorivanovski11@gmail.com

Кључне речи:
Компас, LiDAR, облак тачака, iPhone, пећина

данцима у Македонији. Тродимензионални облаци тачака обрађени су у софтверу CloudCompare, а структурне оријентације добијене су коришћењем алата Virtual Compass. Мерења заснована на смартфону, спроведена на 3D облаку тачака помоћу алата Virtual Compass, показују веома добро слагање са подацима добијеним геолошким компасом, што указује да мобилни LiDAR може представљати поуздану и ефикасну допуну традиционалним теренским методама у пећинским и другим просторно ограниченим окружењима.

Introduction

The rapid advancement of technology and its continuous specialization in specific directions shape the orientation of today's modern world toward an open market society. Consequently, both hardware and software components are primarily developed in response to the need for practical application, among other things, for purely commercial purposes.

With the progress of technology in all spheres of human life, a wide range of tools has emerged. In the fields of construction, geotechnics, and geology, innovative technologies for data acquisition, analysis, and processing are increasingly applied. These include complex systems based on laser scanning technologies, global positioning systems (GPS), and high-performance computer hardware, which, together with continuously evolving software and algorithms, enable efficient data processing and interpretation.

In structural geology, one of the fundamental instruments traditionally used is the geological compass, designed to measure the orientation of geological structures. However, the application of modern Terrestrial Laser Scanners (TLS) now enables the extraction of the same structural information, dip and dip direction, from digital 3D data. The major limitation of these instruments remains their high cost, which motivates users to seek affordable alternatives capable of achieving comparable accuracy.

The introduction of LiDAR (Light Detection and Ranging) technology into smartphones represents a significant innovation. Although LiDAR has long been used commercially on vehicles, drones, and other platforms, its integration into mobile devices marks a new stage in its democratization. In 2020, Apple Inc. released the first smartphone equipped with an advanced LiDAR-based depth sensor and an enhanced augmented reality (AR) application programming interface (API). The main function of this sensor is to measure light distance and capture depth information. While it cannot yet fully replace professional TLS systems, the captured data allow the generation of scaled 3D meshes with realistic geometry and vertical orientation. For the hardware to function effectively, it must be supported by appropriate software applications, which are further discussed in this paper.

Software tools for 3D data processing offer numerous functionalities, enabling the extraction of structural orientations directly from the scanned surfaces. This functionality opens the possibility of using devices such as the iPhone 16 Pro Max as practical instruments for determining the basic geological characteristics of exposed rock formations. The concept of scanning various lithological units using a portable device is changing the way structural geologists acquire the data necessary for their analyses.

In the context of this technology's application, three separate measurement campaigns were previously conducted on structural planes at different rock outcrops across Macedonia (Ivanovski et al., 2023, 2024, 2025). The results obtained from the smartphone-based LiDAR scans were compared to those acquired using the traditional geological compass. These three validation studies produced consistent and reliable results, confirming that the use of this technology provides measurements within an acceptable error range comparable to that of the Clar geological compass.

The aforementioned measurements were carried out on outcrops which represent convex surfaces, captured from all exposed sides. This inspired the idea to test the performance of this technology in a different environment: a cave, representing a con-

cave geological object. In this case, scanning would involve capturing the cave's interior surfaces from multiple viewpoints.

For this purpose, a suitable candidate was found in the "Temna Peštera" (Dark Cave), located near the village of Mrežičko in the municipality of Kavadarci. The cave is developed within massive limestone formations. Scanning inside a cave has its advantages and challenges. Among the advantages is the absence of vegetation, while the main limitations include the lack of natural light, restricted access, and the difficulty of capturing certain sections of the cave. In our case, a small part of the cave, approximately 12 meters in length, was scanned and analyzed.

This approach represents the next stage of a broader research effort to evaluate the potential of the iPhone as a practical and innovative tool in structural geology.

General information about the study area

Dark Cave is situated in the immediate vicinity of the village of Mrezichko, 37 km from the city of Kavadarci, at an elevation of 650 m (Fig. 1).

From the end of the asphalt road, it is reached on foot via a 0.5 km trail that leads through the canyon of the Mrezichka River. The carbonate rocks hosting the cave provide an excellent substrate for the development of karst forms, due to their solubility and the presence of both groundwater and surface water.

The cave interior appears as a long, narrow passage (tube-like) with a whitish-gray rocky surface and a moist floor. The length of the section accessible to visitors is about 120 m, with passage widths varying from 1–7 m and heights from 1–8 m. The cave is described as semi-active: in the first section, few speleothems are formed, whereas in the second section there is clear activity and speleothem development (Fig. 2).

From a geological perspective, the cave is developed in thin to thick-bedded Turonian limestones, locally dolomitized (Pendžerkovski et al., 1970). These rocks are relatively strong and whitish-gray. In tectonic terms, the cave belongs to the southern margin of the Vardar Zone, affected by faults and fracturing. The area represents a contact zone of several geological units, dissected by faults and other tectonic structures such as folds. In the immediate vicinity, Triassic (?) clayey schists, hornfels

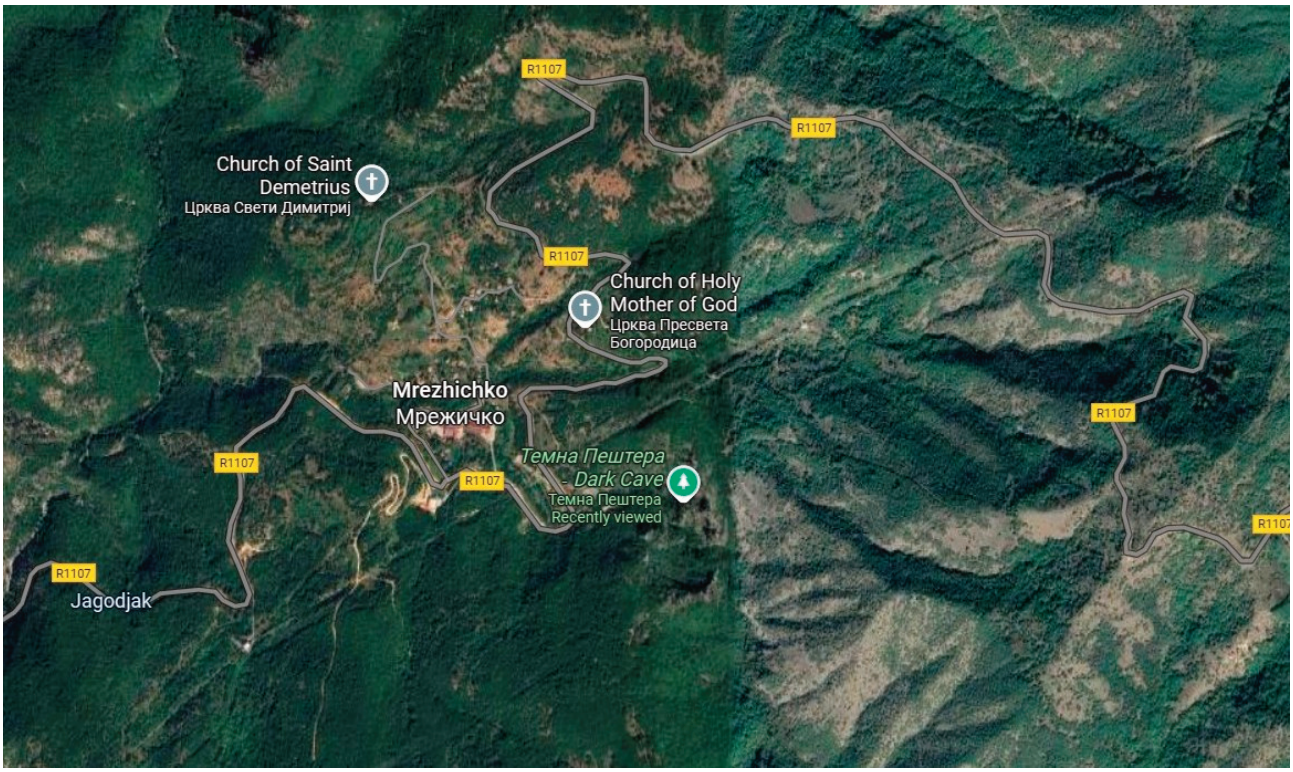

Fig. 1. *Location of the Dark Cave (green mark) (latitude, longitude 41.20493, 22.00268 Google Maps).*

and sandstones, Quaternary brecciated tuffs, and Lower Paleozoic serpentinites and quartzites are observed (Pendžerkovski et al., 1970) (Fig. 3).

Fig. 2. *Interior of the tube-shaped Dark Cave.*

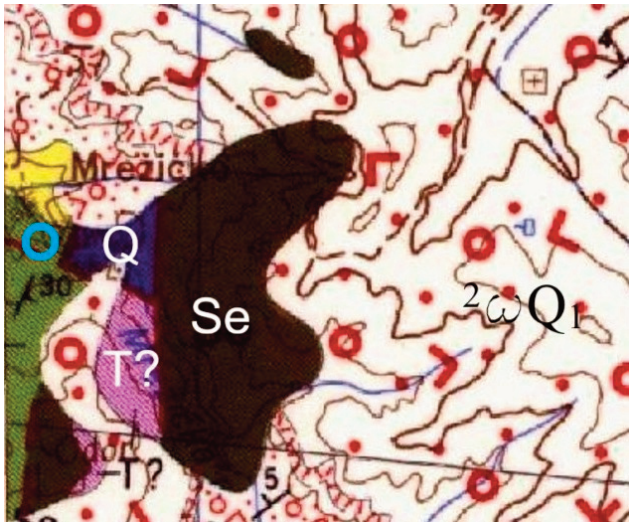

Fig. 3. *Part of geological map (modified after Pendžerkovski et al., 1970), showing the location of the cave indicated with light blue circle.*

The cave formed along a zone of weakness, i.e., a fault line, where karstification was enhanced by water infiltration. The cave itself displays evidence of a variable hydrological regime. During the survey no water was flowing through the passage, although it is evident that at certain times of the year water does flow through it.

The cave developed along a NW–SE-oriented fault zone. The primary conduit follows the main joint system with this orientation, while secondary branches trend orthogonally (NE–SW). It lies within a composite fault-bounded block with offsets, which facilitated infiltration and karst erosion. In several places on the ceiling and walls, fresh microfaults are visible, indicating relatively recent tectonic activity, probably related to post-Paleogene faults that cut the Vardar Zone.

Based on field observations and regarding the geological evolution of this area, it can be stated that during the Jurassic–Cretaceous period, carbonate sediments were deposited in a shallow-marine environment, forming limestones and dolomites. In the Paleogene, tectonic uplift and faulting occurred, opening fractures and initiating karstification. In the Neogene–Quaternary, epigenetic river incision led to the formation of valleys, swallow holes, and caves. At present, the humid climate and periodic flood cycles promote active erosion and calcite precipitation, i.e., hydrogeological processes such as the deposition of secondary carbonates in the form of stalactites and stalagmites.

Used methods, hardware and software

Over the last decade, new high-volume data-acquisition systems, such as remote sensing and geophysical techniques, have generated rich datasets, suggesting that conventional parameter-calculation workflows may be redefined (Riquelme et al., 2018).

Traditional methods rely on direct access to the rock surface; consequently, datasets are often constrained by site accessibility and environmental conditions. Since the 2000s, remote sensing has been applied across multiple fields, notably to the characteri- zation of rock slopes (Riquelme et al., 2021).

In this study, alongside a geological compass, we employ a ground-based 3D laser scanner (terrestrial laser scanner, TLS) to enable a parallel compar-

ison of results. LiDAR surveying yields a 3D point cloud (3DPC) that can be analyzed to detect discontinuity sets, derive their orientations, and extract related geometric parameters (Riquelme et al., 2017). The acronym LASER stands for Light Amplification by Stimulated Emission of Radiation. A laser is a device that emits a beam (or pulse series) of highly collimated, directional, coherent, in-phase electromagnetic radiation. Laser systems enable acquisition of large volumes of 3D information at extremely high recording rates (Jaboyedoff et al., 2012) (Fig. 4).

The dip and dip direction of cave planes were measured with a Clar-type geological compass manufactured by Freiberger Präzisionsmechanik (Germany) (Fig. 5a). According to the manufacturer's specifications for this type of geological compass, the azimuth circle has 2° graduations (readable to ~0.5°), the clinometer has 5° graduations (readable to ~1°), and the directional accuracy is ±0.5° (ASC Scientific, n.d.).

Smartphone measurements were obtained with an iPhone 16 Pro Max (released September 2024). The device represents a relatively inexpensive alternative to current surveying hardware where moderate accuracy is sufficient. Although it does not perform surface scanning in the same way as TLS devices, it can acquire colorized 3D point clouds at practical field scales (Zaczek-Peplinska & Kowalska, 2022; Pluta & Siemek, 2024) (Fig. 5b).

Using the 3D Scanner App (Laan Labs) on the iPhone, a LiDAR scan of the cave interior was performed (Laan Labs, 2021). The application is launched on the phone, and the available area is recorded with the rear LiDAR sensor (adjacent to the camera). During acquisition, the phone is held appro- ximately 0.3–2.0 m from the surface.

For point-cloud analysis, we used the open-source software CloudCompare (CloudCompare, 2024), a 3D point-cloud processing platform that also handles triangular meshes and calibrated images (available for Windows, Linux, nd macOS; developed in C++ with Qt). Structural orientations (dip and dip direction) were extracted with CloudCompare's Virtual Compass tool.

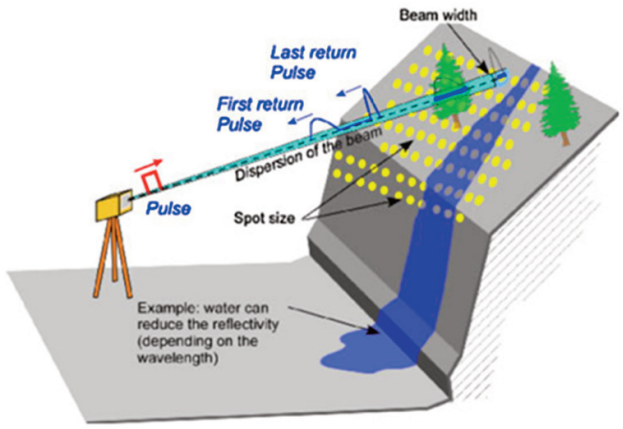

Fig. 4. *Principles of laser scanner data.*

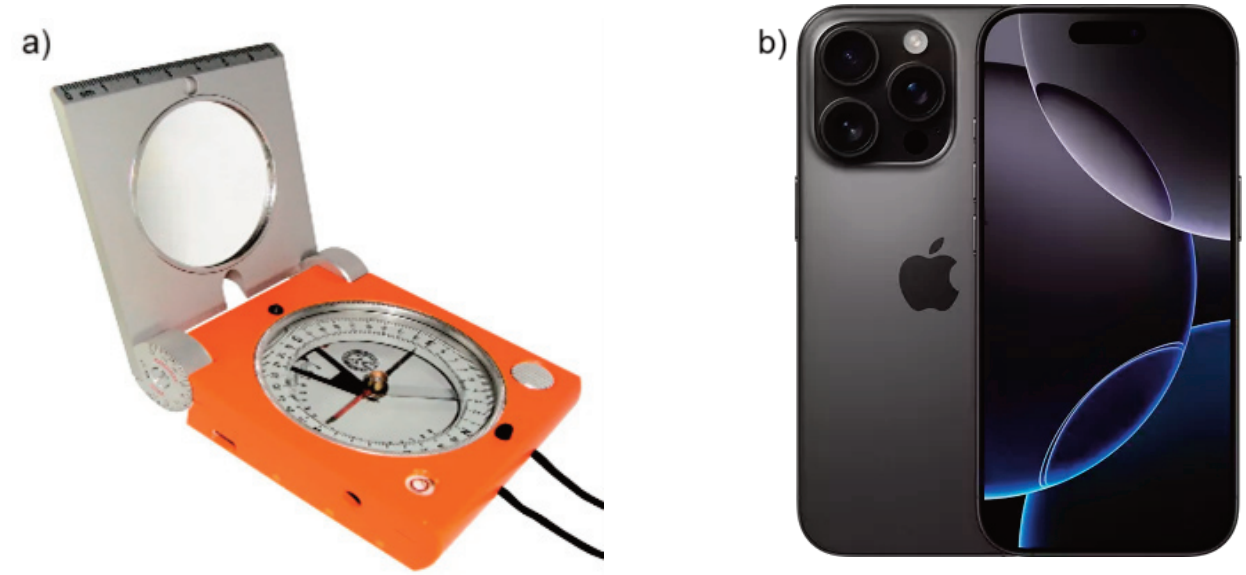

Fig. 5. *Devices used: a) Clar compass; b) iPhone 16 pro Max.*

Data processing

First, measurements were taken with a geological compass. Three readings were acquired at each measurement point because the cave surfaces are not perfectly planar, yielding slightly different values depending on the exact instrument position. In total, 14 points were successfully measured (42 readings). Initially, 16 points were planned, but two could not be relocated on the 3DPC with higher confidence.

After marking each measured location with a colored marker (Fig. 6), smartphone acquisition began. The recording lasted approximately 10 minutes, mainly due to rough terrain and several hard-to-access surfaces.

Fig 6. *Measurement points marked in Dark Cave.*

The recorded 3DPC was exported in.xyz format; the exported file size was 191.25 MB. After loading the point cloud into CloudCompare, it was georeferenced without a precision GPS device, which is not feasible inside the cave. As demonstrated in Ivanovski et al. (2025), manual spatial positioning of the 3DPC is effective; the same approach was adopted here. Only a rotation about the Z-axis was required to expedite scene orientation (Fig. 7).

The raw export contained 5,640,653 points. Following georeferencing and removal of extraneous regions, a working 3DPC of 4,809,630 points was obtained.

Next, using the Virtual Compass tool, the exact field locations were identified on the 3DPC, and three readings per station were performed (Fig. 8).

In total, 14 stations were recorded with the Virtual Compass, i.e., 42 readings, matching the positions measured with the geological compass. As is common on irregular rock surfaces, three readings on the same outcrop segment often yield slightly different values, reflecting local roughness: some areas are relatively planar over broader patches, whereas others display curvature. Care was taken to sample dip and dip direction from all major sectors of the cave (Table 1).

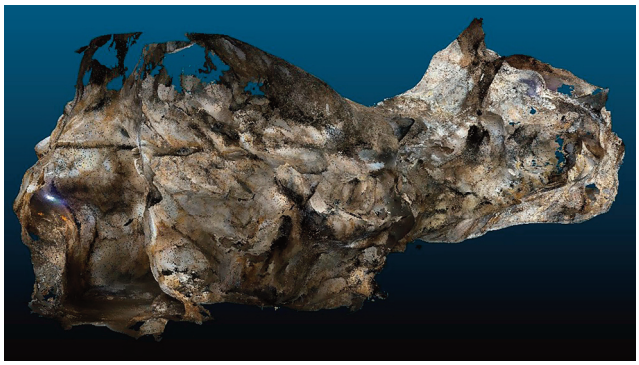

Fig. 7. *Three-dimensional point cloud of a segment of Dark Cave.*

Table. 1. *Dip and dip direction measurements.*

No	Geological compass measurement			Virtual compass measurement		
	1	2	3	1	2	3
1	344/37	333/32	318/38	329/28	321/28	328/31
2	328/13	336/14	315/20	338/22	318/20	324/24
3	321/18	310/25	305/19	317/28	316/28	316/27
4	316/9	312/13	300/8	317/13	311/12	306/10
5	92/41	88/34	92/42	93/42	91/44	91/45
6	345/63	344/68	344/67	337/68	339/65	340/67
7	276/22	275/20	274/22	273/23	278/26	277/33
8	78/78	80/77	80/80	77/77	78/79	78/77
9	86/23	87/22	93/24	83/23	86/23	78/27
10	40/82	42/78	43/79	47/74	48/72	46/75
11	16/88	8/87	16/89	8/85	12/84	8/83
12	153/45	158/40	154/32	155/40	155/38	153/41
13	178/20	163/19	166/17	162/22	163/22	161/24
14	197/39	197/37	186/35	195/43	197/43	197/43

Where planes were smoother, the geological compass and the Virtual Compass results show very similar trends. Conversely, rougher portions exhibited larger deviations in both methods. Overall, the cave's morphology, with gently curved planes shaped by hydrogeological processes, occasionally produced greater within-station variability across the three readings.

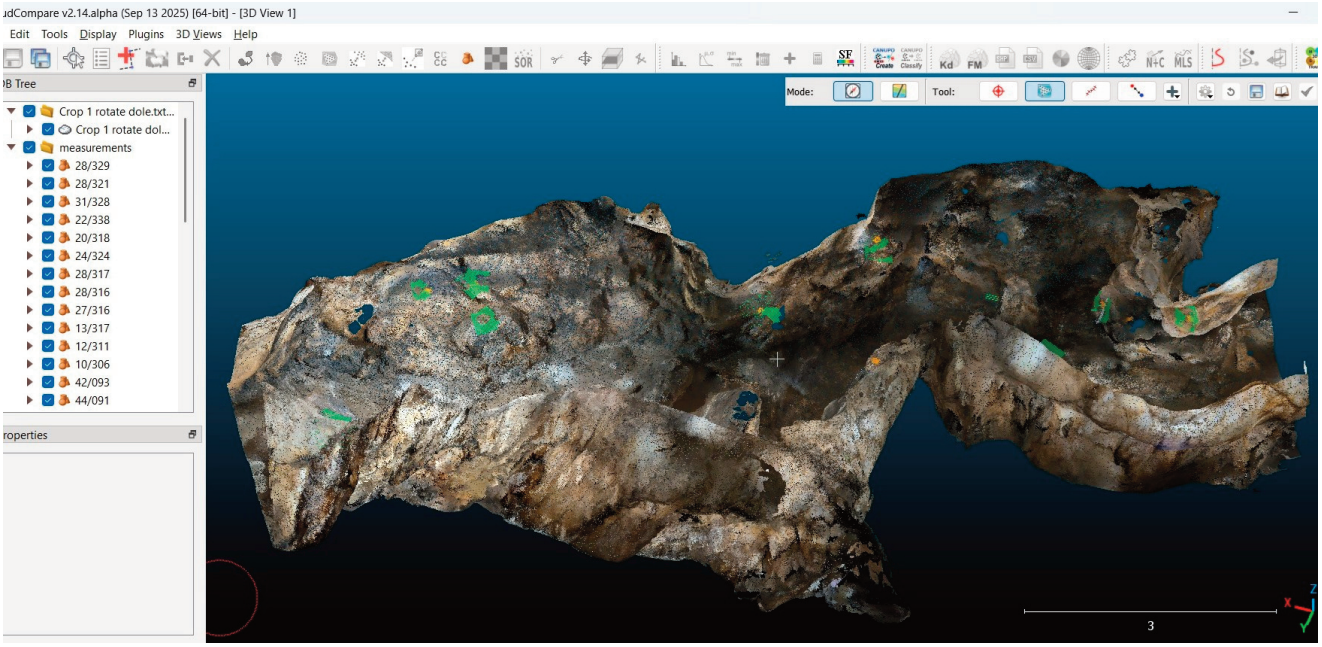

Fig. 8. *Locations of measurements with the virtual compass indicated in green.*

Analysis and results

Analysis of received deviations

When measuring with the geological compass, the maximum difference in azimuth of dip direction for three readings at a single measurement point was 21°, while the maximum difference in dip angle was 13°. For the Virtual Compass, the corresponding maximum differences were 20° and 10°, respectively. These results indicate that the trends of variation are similar for both approaches.

An analysis of the average differences within each set of three measurements at a single point provides additional insights into the compatibility between the two approaches. A frequency analysis of the differences obtained with the geological and the Virtual Compass was conducted to evaluate the distribution of deviations. The difference is expressed as the deviation of the Virtual Compass measurement relative to the geological compass measurement. The average values of differences per point obtained with the Virtual Compass were subtracted from the corresponding average values obtained with the geological compass. (Figs. 9 and 10).

From the results of the dip direction measurements, it can be concluded that all measurements (100.00%) fall within the range of ±8°. Expressed as a percentage, given the possible azimuth range of 0°–360°, this corresponds to a deviation of only 2.22%.

From the results of the dip measurements, it can be concluded that the all measurements (100.00%)

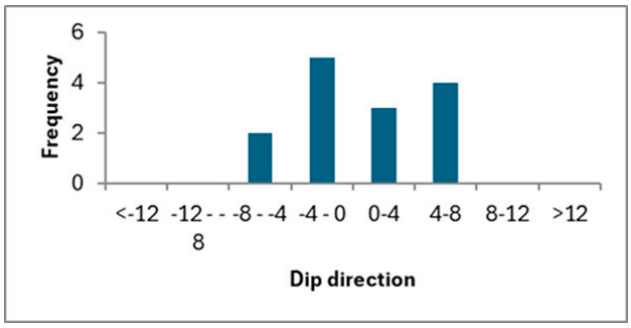

Fig. 9. *Distribution of deviations in dip direction measurements.*

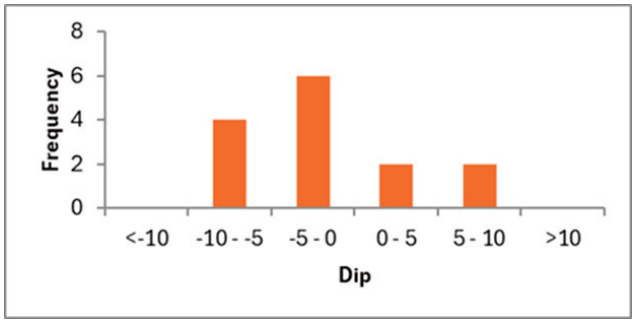

Fig. 10. *Distribution of deviations in dip measurements.*

of deviations fall within ±10°. Expressed as a percentage, given the possible range of 0°–90°, this corresponds to a deviation of 11.11%.

These findings suggest that the obtained statistical results fall within the range of normal deviations.

Regression analysis

To evaluate the relationship between the values of the measured elements obtained by both methods, a regression analysis was performed. This type of analysis enables the research results to be expressed in terms of an analytical relationship or equation. The least squares method was applied as the most suitable approach for establishing the regression dependence.

The coefficient of determination (R^2) was used as an indicator of the strength of the relationship between the variables. The reliability of the regression model is directly related to the magnitude of R^2, which ranges from 0 to 1. The following criteria are commonly applied:

$R^2 < 0.3$: negligible dependence;

$0.3 \leq R^2 < 0.5$: weak correlation;

$0.5 \leq R^2 < 0.7$: moderate correlation;

$0.7 \leq R^2 < 0.9$: strong correlation;

$R^2 \geq 0.9$: very strong correlation.

Thus, a higher value of R^2 indicates a strong relationship between the two variables. In the following (Figs. 11–14), the regression analyses performed for all values obtained from the measurements according to both methods are shown.

Based on the results, it can be concluded that there is a strong dependence between the dip and dip direction values acquired by the two methods. Specifically, the correlation coefficients are as follows:

For all individual measurements: $R^2 = 0.9961$ for dip direction and $R^2 = 0.9649$ for the dip.

For the average values: $R^2 = 0.9988$ for dip direction and $R^2 = 0.9784$ for the dip.

These results clearly demonstrate a very strong correlation between the two approaches, confirming the reliability of smartphone-based LiDAR scanning as a valid alternative to traditional geological compass measurements.

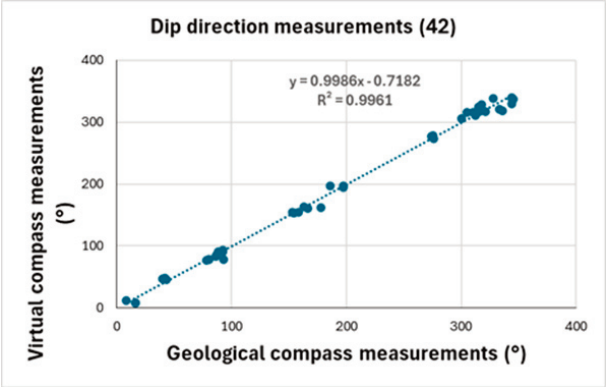

Fig. 11. *Regression analysis from all dip direction measurements.*

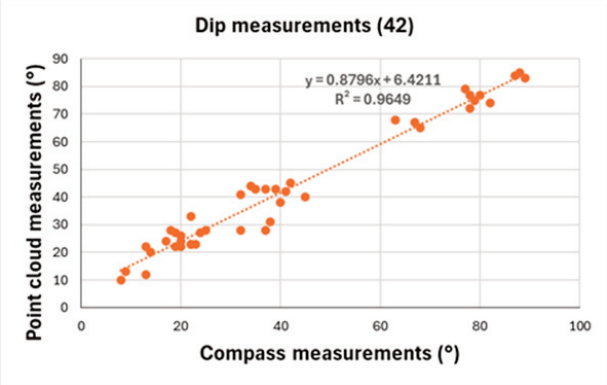

Fig. 12. *Regression analysis from all dip measurements.*

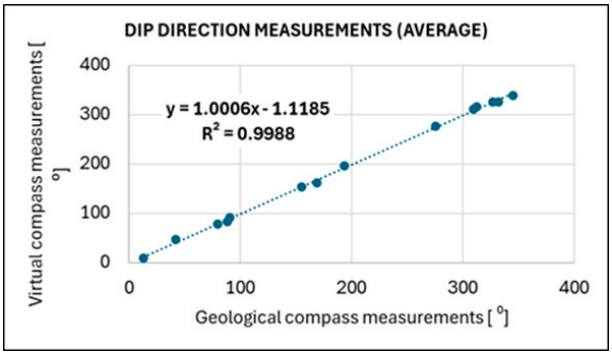

Fig. 13. *Regression analysis from average dip direction measurements.*

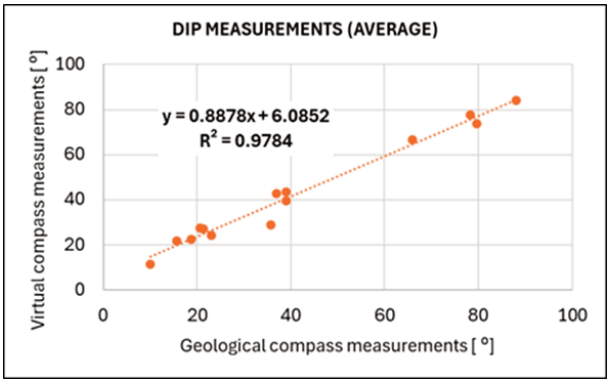

Fig. 14. *Regression analysis from average dip measurements.*

Bland-Altman plot

A Bland–Altman plot is a graphical method used to compare two measurement techniques by plotting the differences between the two methods against their averages. This approach allows for the identification of any systematic bias and provides an assessment of agreement between methods, while also highlighting potential discrepancies (Bland & Altman, 1996).

The principle of the method is straightforward: the X-axis represents the mean of the two measurements, and the Y-axis represents the difference between them. The resulting chart can reveal anomalies; for instance, if one method consistently produces higher values, the data points will appear predominantly above or below the zero line (Kalra, 2017). In the plots presented here, each blue dot corresponds to the difference between two measurements plotted against their average. The red line indicates the mean difference, representing the average bias between the two methods. A mean difference close to zero suggests negligible bias. The upper confidence limit is shown as a blue line and the lower confidence limit as a yellow line, both defined as the mean difference ± 1.96 times the standard deviation of the differences (Figs. 15 and 16).

For both dip direction and dip angle, the majority of data points lie within the limits of agreement, which demonstrates a high level of consistency between the two methods. While a few points appear near or outside the limits of agreement, these outliers may be attributed to measurement errors, extreme values, or other influencing factors. Overall, the plots indicate that the two measurement techniques generally agree well, with most diffe-rences falling within the expected range. The overall agreement is strong, confirming that the methods can be used interchangeably for the majority of measurements.

Display on a stereogram

Doing the analysis, we must bear in mind that together, the dip and dip direction measurements provide a complete description of the orientation of the geological feature. They cannot be condensed into a single number because they represent two distinct aspects of the feature's geometry.

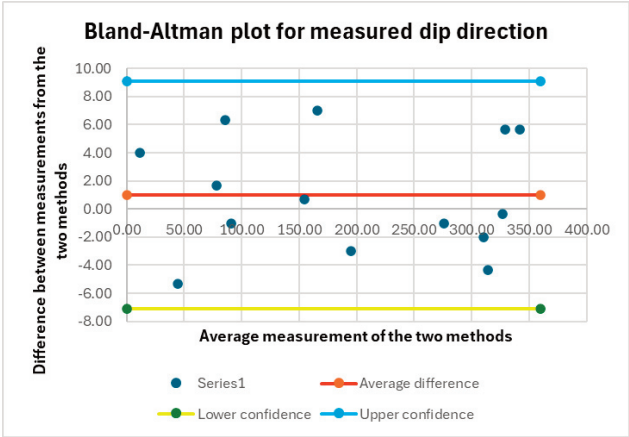

Fig. 15. *Bland-Altman plot for measured dip direction.*

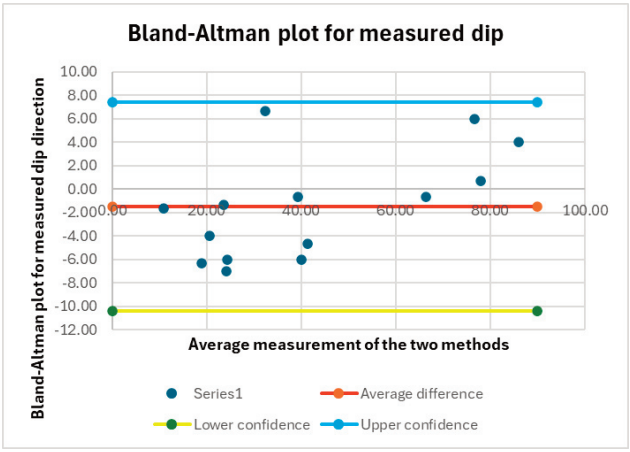

Fig. 16. *Bland-Altman plot for measured dip.*

One way to represent the dip and dip direction together is to show the maximum of poles on stereograms using the software Dips (Figs. 17 and 18).

Looking at these two stereograms, it can be concluded that the resulting poles obtained with geological and Virtual Compass coincide quite well.

Discussion and conclusions

Following a series of successful validations of smartphone-integrated LiDAR for structural-geology applications on various outcrops, we extended the methodology into a cave environment. Dark Cave emerged as a suitable candidate not only for its natural appeal but also for its tube-like geometry and dimensions, which allow nearly all walls to be sur-

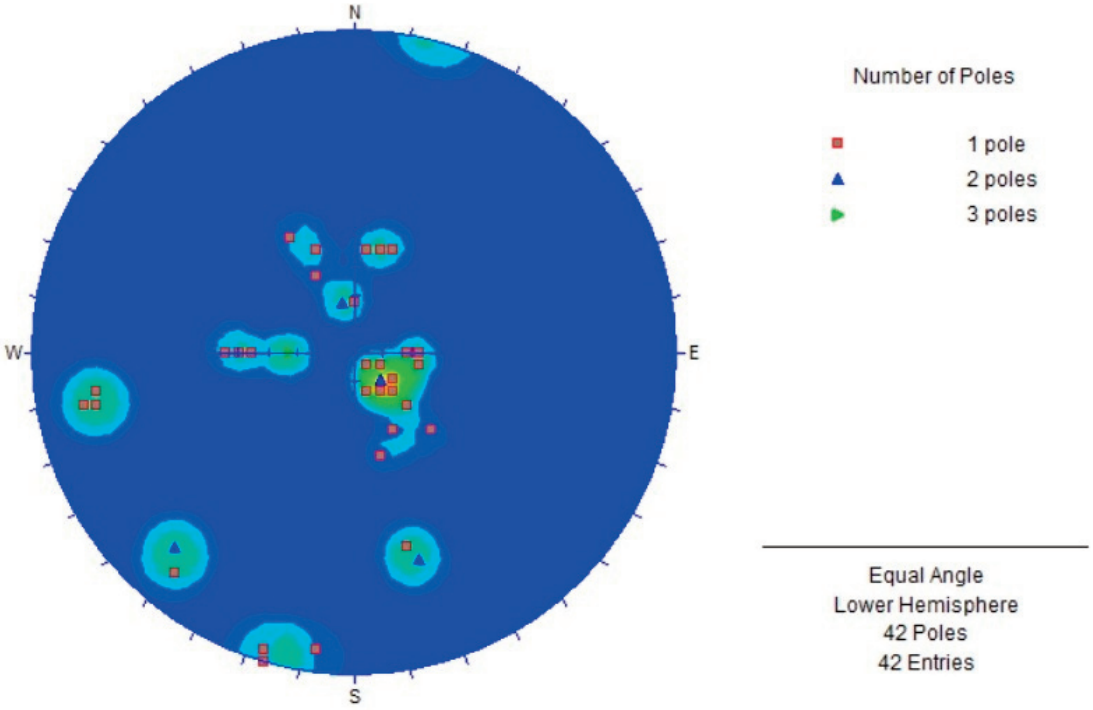

Fig. 17. *Maximum of the poles - geological compass.*

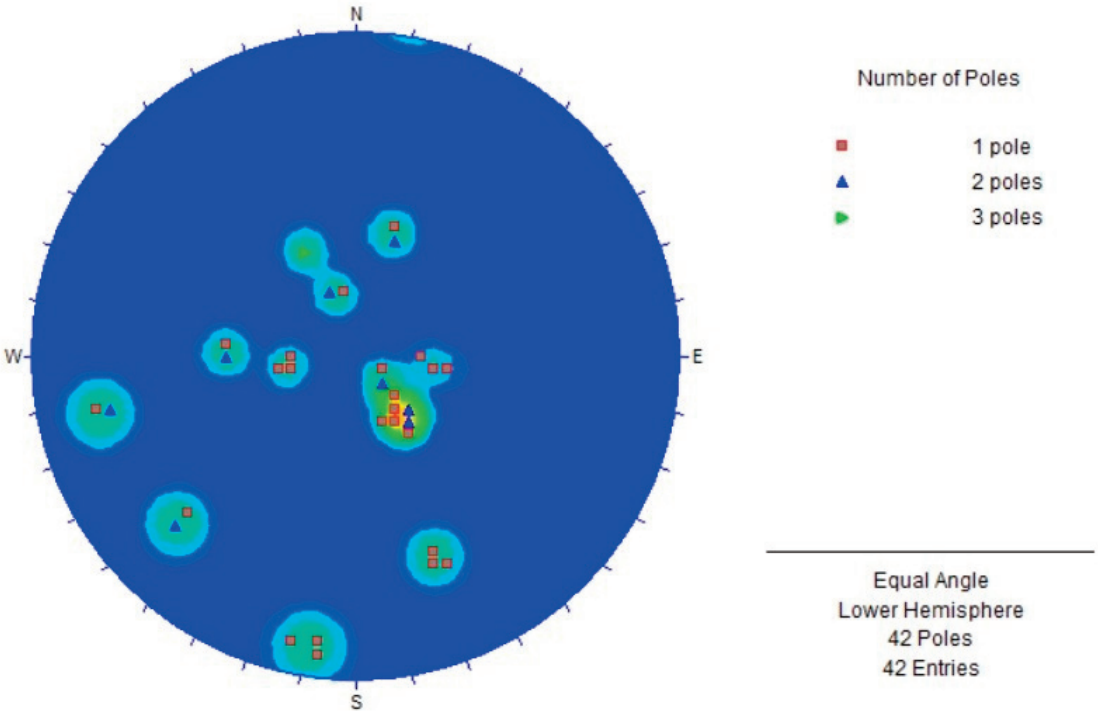

Fig. 18. *Maximum of the poles - Virtual Compass.*

veyed with both a geological compass and a smartphone. For this study, we selected a cave segment representing roughly one-tenth of the total length, large enough to yield a representative 3D point cloud without exceeding the phone's capture capaity. The chosen segment also offered favorable accessibility and planar surfaces appropriate for structural measurements.

A practical challenge was darkness. We therefore employed artificial lighting (fixed lamps plus a moving auxiliary light synchronized with the phone). The resulting point cloud, when compared with scans collected on sunlit outcrops, maintained comparable quality. High humidity hindered secure placement of some markers, and marking the cave walls is not appro-priate; consequently, a few survey stations could not be confidently relocated in software. With more meticulous preparation and enhanced lighting, even better results, and more stations, can be expected. In this trial, we completed 14 stations (i.e., 42 readings).

A first-pass visual comparison of dip/dip-direction from the geological compass versus the Virtual Compass reveals a consistent trend of agreement. For specific surfaces, the within-station spreads across the three readings are similar between both methods, primarily because most cave wall "planes" are not perfectly planar but gently curved due to hydrogeological processes. Even so, a recognizable pattern of correspondence emerges between the instruments.

We then performed formal analyses using multiple independent methods.

The distribution of deviations shows that, although a few stations exhibit larger within-station differences, the overall spread is consistent with what experienced geologists routinely observe with a traditional compass. Deviations are generally larger for dip angle than for azimuth, reflecting both the smaller numerical range (0–90° vs. 0–360°) and the finer tick marks on the compass scale used for dip (Ivanovski et al., 2023, 2024, 2025).

Regression analysis, as in our previous three outcrop studies, yielded stable and very high R^2 values, indicating a strong correlation between approaches (geological compass vs. Virtual Compass on a phone-derived 3D point cloud).

The Bland-Altman plots, widely used in medical method-comparison studies, also proved useful here: for both dip and dip direction, the vast majority of measurements lie within the limits of agreement, supporting a high level of consistency and confirming that the two methods can be used in parallel.

While the above analyses compare like-for-like variables (dip direction vs. dip direction; dip vs. dip), the most comprehensive visualization of the measurement "package" is via stereographic projection of pole maxima. This representation likewise shows excellent coincidence between the two methods.

Overall, the evidence indicates that the modern, low-cost technologies employed here are consistent with results obtained by an experienced geologist using a traditional compass. Multiple analytical viewpoints show high concordance between methods. Given that the advantages outweigh the limitations, the Virtual Compass can be considered a valid alternative to traditional structural measurements with a geological compass.

It remains essential for engineers and scientists to continue refining this mode of structural data acquisition and to stay open to new technologies that can be integrated into geology. Naturally, technology cannot replace expertise: geological insight and understanding of fundamental processes are indispensable when working with both traditional and modern tools.

Acknowledgments

We sincerely thank Dr. Ana Mladenović, Dr. Aleksandar Petrović and Dr. Nevenka Đerić for their valuable comments and suggestions, which enhanced the quality of this manuscript.

References

ASC Scientific. (n.d.). ASC Scientific. Retrieved November 11, 2025, from https://www.ascscientific.com/

Bland, J. M . & Altman, D. G. 1996. Statistics notes: measurement error. *BMJ*, 312 (7047): 1654. doi:10.1136/bmj.312.7047.1654.

CloudCompare, 2024. CloudCompare: 3D point cloud and mesh processing software. Retrieved October 10, 2025, from https://www.cloudcompare.org.

Ivanovski, I., Nedelkovska, N., Petrov, G., Jovanovski, M. & Nikolovski, T. 2023. Comparison between traditional and contemporary methods for data recording in structural geology. *Geologica Macedonica*, 37 (2): 119–133. https://doi.org/10.46763/GEOL23372119i.

Ivanovski, I., Maksimov, B., Petrov, G., Dimov, G., Jovanovski, M. & Nedelkovska, N. 2024. Using the iPhone as a tool in structural geology. *Proceedings of the 5th Congress of the Geologist of the Republic of Macedonia, Ohrid, 27-29 September 2024*, 285-292.

Ivanovski, I., Dimov, G., Nedelkovska, N., Petrov, G. & Jovanovski, M. 2025. Application of Smartphone LiDAR Technology for Road Slope Monitoring. *Proceedings of the Third Macedonian Road Congress*, *Skopje, 6-7 Setember, 2025*, p. 97.

Jaboyedoff, M., Oppikofer, T., Abellán, A., Derron, M., Loye, A., Metzger, R. & Pedrazzini, A. 2012. Use of LIDAR in landslide investigations: a review. *Natural Hazards*, 61 (1): 5–28.

Kalra, A. 2017. Decoding the Bland–Altman plot: Basic review. *Journal of the Practice of Cardiovascular Sciences*, 3: 36. 10.4103/jpcs.jpcs_11_17.

Laan Labs, 2021. 3D Scanner App - LiDAR Scanner for iPad & iPhone Pro. Retrieved October 10, 2025, from https://www.3dscannerapp.com.

Pendžerkovski, J., Rakičević, T., Ivanovski, T. & Guzelkovski, D. 1970. Osnovna geološka karta SFRJ 1:100 000. Tumač za list Kožuf K34 – 105 [*Basic Geological Map of Socialist Federal Republic of Yugoslavia 1:100 000. Explanatory booklet for the Sheet* Kožuf – in Macedonian]. Geološki zavod, Skopje.

Pluta, P. & Siemek, D. 2024. Possibilities and limitations of using iPhone 13 Pro with built-in LiDAR sensor in cave research – on the example of paleoflow analysis in Mylna Cave (Western Tatra Mts, Poland). *Landform Analysis*, 42: 51–62. DOI: 10.12657/landfana-042-004.

Riquelme, A., Cano, M., Tomás, R. & Abellán, A. 2017. Identification of Rock Slope Discontinuity Sets from Laser Scanner and Photogrammetric Point Clouds: A Comparative Analysis. *Procedia Engineering*, 191: 838–845.

Riquelme, A., Tomás, R., Cano, M., Pastor, J.L. & Abellán, A. 2018. Automatic Mapping of Discontinuity Persistence on Rock Masses Using 3D Point Clouds. *Rock Mechanics and Rock Engineering*, 51 (10): 3005–3028.

Riquelme, A., Tomás, R., Cano, M., Pastor, J.L. & Jordá-Bordehore, L. 2021. Extraction of discontinuity sets of rocky slopes using iPhone-12 derived 3DPC and comparison to TLS and SfM datasets. *IOP Conf. Series: Earth and Environmental Science*, 833: 012056.

Zaczek-Peplinska, J. & Kowalska, M. 2022. Evaluation of the LiDAR in the Apple iPhone 13 Pro for use in Inventory Work. *FIG Congress 2022, Volunteering for the future - Geospatial excellence for a better living, Warsaw, Poland, 11–15 September 2022*, 19pp.

Резиме

Прикупљање структурних података у пећини коришћењем LiDAR-а на паметном телефону и алата Virtual Compass

Приступачно 3D снимање мења токове рада у структурној геологији, који су некада били доминантно засновани на терестричком ласерском скенирању (TLS). Надовезујући се на низ валидација на изданцима у Македонији (2023–2025), постављамо питање да ли LiDAR на паметном телефону, конкретно iPhone 16 Pro Max, може да обезбеди поуздана мерења пада и правца пада са конкавних зидова пећине и колико се она подударају са опажањима помоћу геолошког компаса типа Clar.

Истраживање је спроведено у Тамној пећини код Мрежичка, Кавадарци, која је формирана у танко- до дебело слојевитим кречњацима у оквиру тектонски контролисаног канала. Одабрали смо унутрашњи сегмент од 12 m, отприлике једну десетину доступне дужине, јер нуди разуман приступ и довољно равне површине за структурна очитавања. Теренска контрола обухватила је 14 станица са по три очитавања компасом на свакој (Freiberger Clar тип), што је укупно дало 42 мерења. Паралелно је урађено LiDAR скенирање паметним телефоном коришћењем апликације 3D Scanner, а подаци су обрађени у CloudCompare-у. Извезени .xyz облак тачака (191,25 MB) садржао је 5.640.653 тачака; након обрезивања и ручног георефернцирања прилагођеног пећинском окружењу,

радни облак имао је 4.809.630 тачака, при чему је сцена оријентисана једноставном ротацијом око Z -осе.

Структурне оријентације затим су извучене из облака тачака помоћу CloudCompare алата Virtual Compass на истих 14 станица (опет 42 очитавања). Пошто су пећински зидови обично благо закривљени, узимање по три очитавања на свакој станици са оба инструмента помогло је у бележењу локалне храпавости: распони унутар станица достизали су 21°/13° (азимут/пад) за Clar компас и 20°/10° за Virtual Compass. Упркос овој очекиваној микро-варијабилности, све разлике у правцу пада биле су унутар ±8° (2,22% од 0–360°), а све разлике у паду унутар ±10° (11,11% од 0–90°).

Више линија анализе указује на снажно слагање између метода. Резултати регресије показују веома високе коефицијенте детерминације: R^2 = 0,9961 (правац пада) и 0,9649 (пад) за сва појединачна очитавања; R^2 = 0,9988 и 0,9784 за просеке станица, што указује на одличну линеарну везу. Bland-Altman дијаграми позиционирају велику већину тачака унутар граница слагања за обе променљиве, сугеришући занемарљиву пристрасност и практичну заменљивост. Коначно, стереографске пројекције (максимум полова) из компаса и Virtual Compass скупа очитавања блиско се поклапају, додатно потврђујући конзистентност оријентација.

У оперативном смислу, пећинско окружење наметнуло је позната ограничења: мрак је захтевао фиксно и помично вештачко осветљење, док је влага отежавала пријањање маркера и изазвала неколико неизвесности при релокацији у софтверу. Ипак, радни ток заснован на паметном телефону произвео је колорисан 3D облак тачака довољног квалитета за структурну анализу и упоредив, у смислу намене, са резултатима претходно добијеним на осунчаним изданцима.

Заједно, ови резултати показују да у конкавном, слабо осветљеном пећинском окружењу LiDAR на паметном телефону у комбинацији са Virtual Compass алатом даје структурне оријентације које се веома добро поклапају са мерењима помоћу Clar компаса. С обзиром на високе R^2 вредности, слагање према Бланд–Алтман анализи и стереографској кохеренцији, мобилни LiDAR представља поуздану, нискобуџетну допуну, а у многим случајевима и одрживу алтернативу традиционалним теренским методама за структурно приступачне пећинске зидове и друга ограничена геолошка окружења.

Manuscript received November 01, 2025
Revised manuscript accepted November 17, 2025